crystals

MDPI

Article

Comparison of the Ionic Liquid Crystal Phase of $[C_{12}C_1im][BF_4]$ and $[C_{12}C_1im]Cl$ by Atomistic MD Simulations

Giacomo Saielli [1,2]

[1] CNR Institute on Membrane Technology, Via Marzolo, 1 – 35131 Padova, Italy; giacomo.saielli@cnr.it
[2] Department of Chemical Sciences, University of Padova, Via Marzolo, 1 – 35131 Padova, Italy

Received: 12 March 2020; Accepted: 26 March 2020; Published: 27 March 2020

Abstract: We present fully atomistic molecular dynamics (MD) simulations at 450 K of two ionic liquid crystals in the smectic phase: 1-dodecyl-3-methylimidazolium tetrafluoroborate ($[C_{12}C_1im][BF_4]$) and 1-dodecyl-3-methylimidazolium chloride ($[C_{12}C_1im]Cl$). The two systems experimentally exhibit different ranges of thermal stability of the ionic smectic phase: The chloride salt has a more stable LC phase, between 270.3 K and 377.6 K, with a range of SmA of more than 107 K. In contrast, the tetrafluoroborate salt has a smectic phase between 299.6 K and 311.6 K, with a range of mesophase of just 12 K. The MD simulations show that the chloride system is stable in the smectic phase for the 5 ns of simulation, while the tetrafluoroborate salt melts into an isotropic ionic liquid, in qualitative agreement with the experiments. Comparison of the electrostatic and van der Waals energetic contributions enables one to rationalize the observed behavior as being due to the large size of the $[BF_4]$ anion: a larger size of the anion means a lower charge density, and therefore a weaker electrostatic interaction in the ionic layer.

Keywords: ionic liquid crystals; molecular dynamics simulations; ionic liquids; electrostatic interactions; van der Waals interactions; anion size

1. Introduction

Ionic liquid crystals (ILCs) are materials formed by ions and exhibiting thermotropic liquid crystal (LC) behavior; that is, the mesophases are observed as a function of the temperature for the pure samples [1,2]. They are promising materials for applications wherein an anisotropic conduction of charge and/or matter is sought; for example, Li-ion batteries [3] and dye sensitized solar cells (DSSC) [4–6]. From an experimental point of view, several kinds of ILCs have been synthesized since the first consistent report of the properties of long-chain imidazolium salts [7], though ILCs have actually been around since immemorable time, given that metal alkanoates, i.e., soaps, have ionic liquid crystalline phases [8–10]. Inclusion of photo or electrochromic moieties in the molecular structure results in materials with interesting optical properties; for example, an increased optical Kerr effect [11], and the possibility of preparing electrochromic smart materials and devices [12–18].

Usually, ILCs are composed of an organic cation and an inorganic anion, as found in ionic liquids (ILs): besides the already mentioned imidazolium cations, several other systems have been investigated, such as guanidinium [19,20], pyrrolidinium [21] and bipyridinium (viologens) [22–28]. In all cases, the key molecular feature which is necessary in order to have ionic liquid crystal behavior is a relatively long alkyl chain attached to the ionic part. This will guarantee nano-segregation between the ionic parts and the hydrophobic chains, leading, almost invariably, to layered, that is smectic, ILC phases, wherein ionic layers are alternated with hydrophobic alkyl layers, though no positional order exists within each layer. A few years ago, Nelyubina et al. reported an interesting correlation, experimentally

determined, between the minimum chain length required to observe ILC mesophase and the relative volume between 1-alkyl-3-methylimidazolium cations and several anions [29]. They observed that, the larger the anion, the longer the alkyl chain has to be in order to have an ionic smectic phase. For example, while imidazolium chloride salts have a ILC phase already with a C12 alkyl chain, at least C14 is needed when the anion is the larger PF_6^- and a C22 alkyl chain is needed for the case of bistriflimide ($(CF_3SO_2)_2N^-$) anion [29]. A similar behavior is observed in metal alkanoates: when the anion bearing the alkyl chain is paired with larger cations (e.g., from Li^+ to Cs^+) a longer alkyl chain is needed in order to observe the formation of ILC phases [30–32].

Computer simulations are a very useful tool with which to investigate the microscopic features of complex fluids. ILCs have been the subjects of several of such investigations with a variety of force field types: fully atomistic [33–38], coarse-grained [39–41] and highly coarse-grained [42–46]. In a recent combined experimental and simulation study, we investigated in detail the effect of the relative anion size on the thermal range of stability of the ionic smectic phase of a series of *N*-alkyl-3-methylpyridinium halides and trihalides [47]. In that work, we proposed that the stability of the ionic smectic phase is governed by a balance between the energetic stability of the two alternating layers, the ionic and the hydrophobic one: it is possible to destabilize one layer, for example, the ionic layer, by making the anion larger (so that the charge density is lower and therefore the electrostatic interaction is weaker) without destroying the ionic smectic phase, provided that we increase the stability of the hydrophobic layer, mostly due to van der Waals interaction, by increasing the chain length. Similarly, in a pure computational study [48] we observed that increasing the electrostatic interaction by artificially increasing the charge of the ions does increase the thermal range of stability of the ionic smectic phase by increasing the clearing point (smectic-to-isotropic transition) with a very minor effect on the crystal-to-smectic transition temperature [48].

In this work we extend our previous investigation with a direct comparison of two imidazolium ionic liquid crystals, 1-dodecyl-3-methylimidazolium tetrafluoroborate ($[C_{12}C_1im][BF_4]$) and 1-dodecyl-3-methylimidazolium chloride ($[C_{12}C_1im]Cl$). The two systems experimentally exhibit ionic smectic phases with different thermal ranges of stability: the chloride salt has a wide range for its SmA phase of more than 107 K, from 270.3 to 377.6 K [49], while the tetrafluoroborate salt has a much narrower range of mesophase of just 12 K, from 299.6 to 311.6 K [50]. The rather close crystal-to-smectic melting temperatures and the significantly different smectic-to-isotropic clearing points suggest that the different anions affect mostly the stability of the smectic phase compared to the isotropic liquid, while the stability of the crystal phase is less affected, in agreement with the suggestions of the coarse-grained simulations of reference [48]. Herein, using fully atomistic MD simulations, we study the structures of the two title systems at 450 K. The results show that the electrostatic contribution and the van der Waals contribution are significantly different in the two systems and can explain the different thermal ranges of stability of the ionic smectic phases in the two systems.

2. Materials and Methods

Simulations were run with the software DL_POLY Classic [51] using the fully atomistic, non-polarizable, CL&AP Force Field for ionic liquids [52]. Initial boxes were the ones of reference [36] (after removing the probe molecule of dichlorobenzene); thus, both consisted of 511 ion pairs. The simulations were run at 450 K for 5.1 ns in the NPT ensemble. The time step was set to 1 fs; the electrostatic interactions treated with the Ewald sum method with a precision of 10^{-6}. All C–H bonds were constrained. Temperature and pressure were controlled with the Hoover thermostat and barostat [53,54], and the equation of motion was integrated using the *leapfrog* algorithm [55] with a *shake* algorithm to constrain C–H bonds (tolerance 10^{-8}) [56,57]. Structures and configurations were visualized with VMD software [58].

The choice of the simulation temperature, higher than the clearing point for both systems, was dictated by the following reason: it is widely acknowledged that non-polarizable force fields, like the one used here, overestimate the electrostatic interaction [59,60]. While the structural properties

are generally good, the dynamics are significantly slowed down. A secondary effect of the increased electrostatic interaction is an increase of the transition temperatures observed in the simulations [37]. A common workaround is to use higher temperatures to speed up the sampling of the phase space. This approach has been used in our previous works, and the comparison with experimental results was qualitatively very good, though the temperatures of the simulations were not the same as the ones of the experiments [47,61]. Moreover, for a qualitative understanding, the most important point is that the two systems are simulated at the same temperature, so that the comparison will be meaningful. Thus, using a higher temperature, as mentioned, allows one to speed up the dynamics, thereby reducing the computational demand, without losing any structural information. We mention here, for the sake of completeness, that another option would be to rescale the total charge by a factor around 0.8, depending on the particular scheme, so that the cation and the anion have total charges of $+0.8e$ and $-0.8e$, respectively [62–64]. This, of course, lowers the electrostatic interaction, somehow mimicking the effect of polarizability. A thorough comparison of polarizable and non-polarizable force fields with scaled charged is reported in reference [65]. In this work, in keeping with our previous studies, we have preferred to use a higher temperature rather than scaling the charges.

3. Results

As mentioned in the Materials and Methods section, both simulations started from the final configurations used in [36] after removing the solute dichlorobenzene molecule, since here we are interested in the bulk properties only. It is worth remembering that, for $[C_{12}C_1im][BF_4]$, the temperature used in [36] was 350 K in order to keep the smectic phase stable. Here we suddenly increased the temperature to 450 K—the same T used for the system $[C_{12}C_1im][Cl]$. As we can see in Figure 1, the tetrafluoroborate system is initially in the smectic A phase, but after 5 ns it appears completely isotropic with no evidence of layers. In contrast, see Figure 2, the layered structure of the chloride salt is clearly maintained unaltered during the simulation.

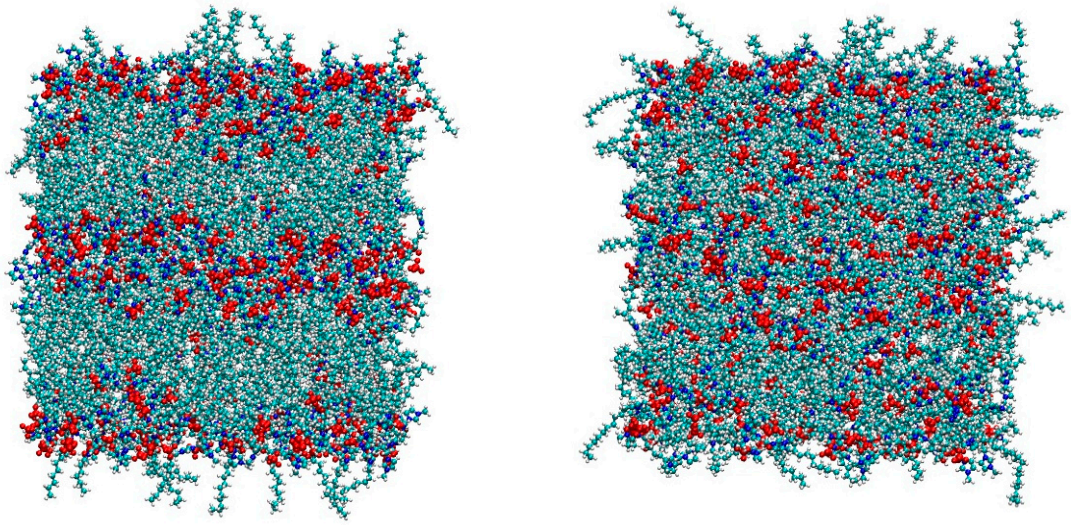

(**a**) (**b**)

Figure 1. (**a**) Initial (t = 100 ps) and (**b**) final (t = 5 ns) snapshots of the simulation box of $[C_{12}C_1im][BF_4]$ at 450 K. Color code: cyan: carbon; white: hydrogen; blue: nitrogen; red: $[BF_4]^-$.

A more quantitative information is obtained by comparing the profile of the probability density of the anion center of mass along the director (here oriented along the z axis of the box) at the beginning of the simulation and at the end (see Figure 3 and its caption for more details). Consistent with the snapshots in Figures 1 and 2, the profile for the tetrafluoroborate salt at the beginning shows a clear alternation with the maxima identifying the ionic layers and the minima corresponding to the

hydrophobic layers. However, the density profile at the end of the simulation is clearly flat (within the high noise due to the limited statistics). Again, the analogous curves for the chloride salt indicate first of all a higher degree of positional order, as already discussed in [36], and more importantly, a perfect overlap of the density profiles obtained at the start and at the end of the simulation.

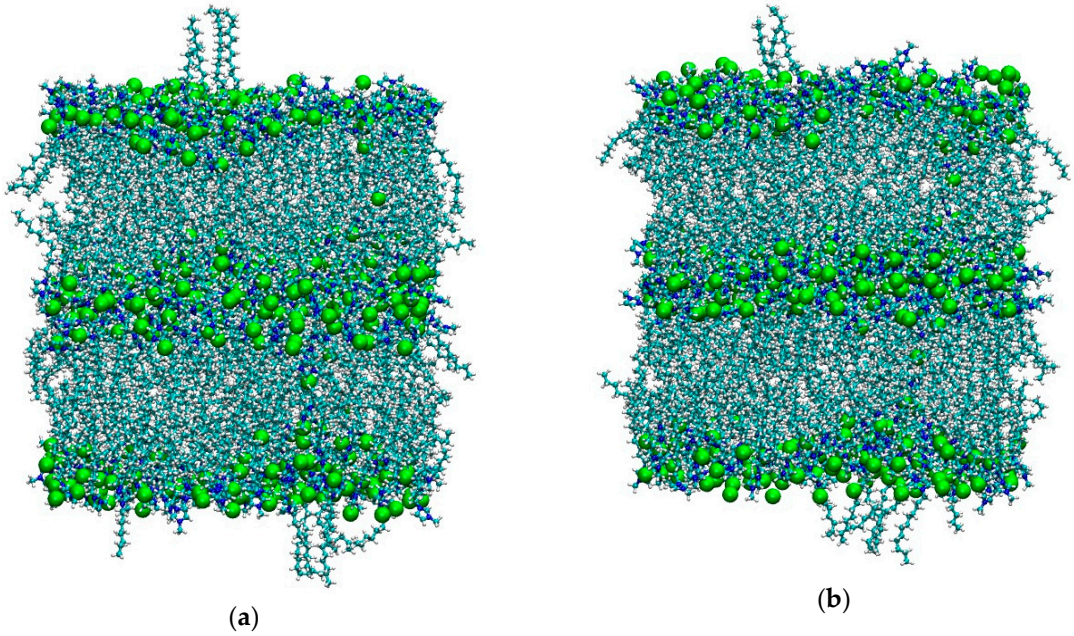

(**a**) (**b**)

Figure 2. (**a**) Initial (t = 100 ps) and (**b**) final (t = 5 ns) snapshots of the simulation box of $[C_{12}C_1im]Cl$ at 450 K. Color code: cyan: carbon; white: hydrogen; blue: nitrogen; green: Cl^-.

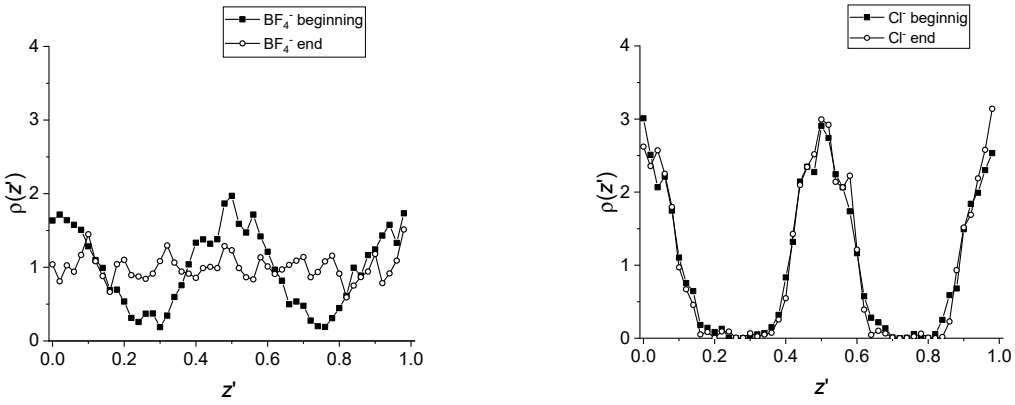

(**a**) (**b**)

Figure 3. Anion's density profile along the director. The abscissa is defined as $z' = z/L_z$, where z is the coordinate along the director of the reference atom and L_z is the box size length along the director. For each timestep, z' is calculated using the instantaneous value of the box size. (**a**) Density profile of the B atom of the anion in $[C_{12}C_1im][BF_4]$ obtained by averaging 1900 snapshots from (solid squares) t = 5 ps until t = 100 ps and from (empty circles) t = 5005 ps until t = 5100 ps. (**b**) Density profile of the Cl^- anion in $[C_{12}C_1im]Cl$ obtained by averaging 1900 snapshots from (solid squares) t = 5 ps until t = 100 ps and from (empty circles) t = 5005 ps until t = 5100 ps.

To conclude this structural analysis, in Figure 4 we report the radial distribution functions of the distance between the geometric center of the imidazolium ring and the anion. As observed already, for $[C_{12}C_1im][BF_4]$ there is a clear difference in the $g(r)$ calculated at the beginning and at the end of the simulation. While the first peak remains very similar in position, amplitude and width, the second and third peaks change significantly, decreasing in intensity as a result of an increased

disorder in the average structure. In contrast, the radial distribution functions of $[C_{12}C_1im][Cl]$ are almost perfectly overlapped.

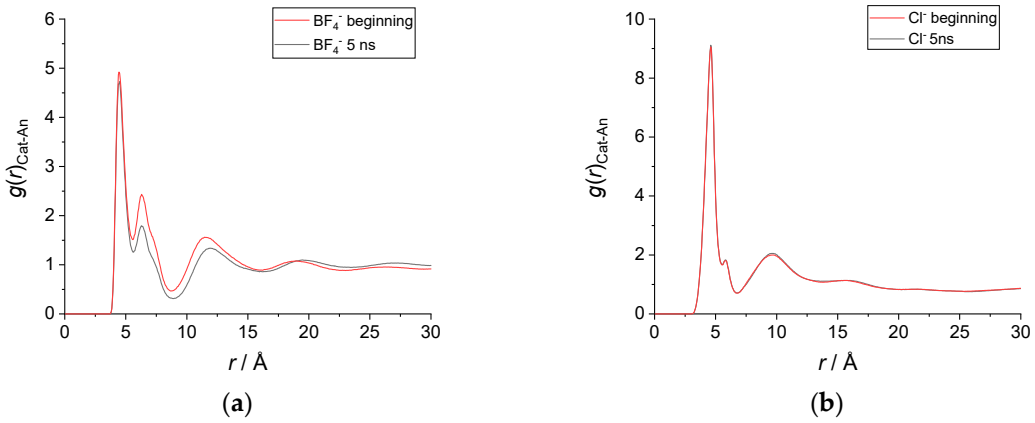

Figure 4. Radial distribution functions—$g(r)$ of the distance between the imidazolium ring's geometric center and the anion center of mass. (**a**) $g(r)$ in $[C_{12}C_1im][BF_4]$ obtained by averaging 1900 snapshots from (red) t = 5 ps until t = 100 ps and from (black) t = 5005 ps until t = 5100 ps. (**b**) $g(r)$ in $[C_{12}C_1im]Cl$ obtained by averaging 1900 snapshots from (red) t = 5 ps until t = 100 ps and from (black) t = 5005 ps until t = 5100 ps.

To summarize the results obtained so far—it is clear that while $[C_{12}C_1im][Cl]$ at 450 K is in a smectic A phase, stable and with well separated ionic and hydrophobic layers, the smectic phase of $[C_{12}C_1im][BF_4]$ at the same temperature is not stable and it undergoes a quick melting into a nano-segregated isotropic liquid during the 5 ns of simulations.

To get some more insights into the phase transition process and the factors that determine the different stabilities of the smectic phase in the two salts, in Figure 5 we show the different contributions of the intermolecular potential energy, the van der Waals term and the Coulomb term, during the 5 ns of simulation. We have removed the first 50 ps from the graph taken as equilibration needed to cancel the effect of the removal of the solute molecule from the starting boxes (see Materials and Methods)

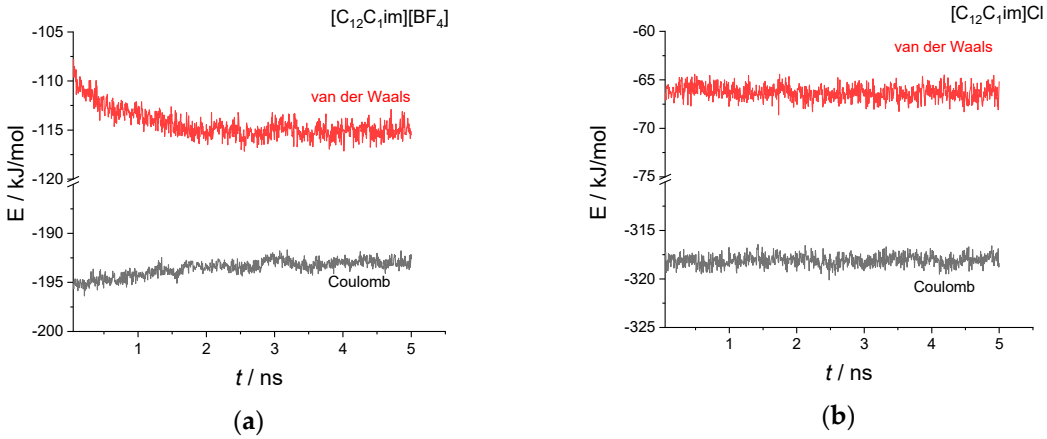

Figure 5. Time evolution of the two intermolecular energy contributions, van der Waals and Coulomb, during the 5 ns simulation for the two systems investigated: (**a**) $[C_{12}C_1im][BF_4]$; (**b**) $[C_{12}C_1im]Cl$.

Clearly, the tetrafluoroborate salt is not at the equilibrium and we can see a drift of the energies that lasts for about 3 ns. The Coulomb energy increases (becomes less negative), while the van der Waals energy decreases (becomes more negative). We should stress here that the Coulomb energy is essentially due to the electrostatic interaction involving the imidazolium ring and the anion, with a negligible contribution from the alkyl chains. In contrast, the van der Waals interaction has a major contribution

from the hydrophobic alkyl chains but also non-negligible contributions from the imidazolium ring and the anions. At variance with the tetrafluoroborate salt, for the chloride salt we note a constant trend of both energy contributions during the 5 ns simulation, indicating an equilibrium condition.

4. Discussion

Comparison of the energetic contributions, see Table 1, reveals that the stable smectic phase of the chloride salt is characterized by a weaker van der Waals (vdW) interaction compared to the tetrafluoroborate salt. This can be indeed partly attributed to the larger number of atoms per mole of tetrafluoroborate salt (five atoms in the $[BF_4]^-$ anion vs. just one for the chloride). In contrast, the Coulomb contribution is significantly larger (that is, more negative) in the chloride salt and overcompensate for the weaker vdW contribution. This increased electrostatic interaction is certainly the result of a much more concentrated negative charge in a relatively small anion that allows the cation-anion interaction to be stronger.

Table 1. Average intermolecular energetic contributions for the two systems investigated, in kJ/mol.

	E Coul	**E vdW**
$[C_{12}C_1im][BF_4]$	−193.0 ± 9.6 (~ −195) [1]	−115.1 ± 5.7 (~ −110) [1]
$[C_{12}C_1im]Cl$	−318.0 ± 15.9	−66.4 ± 3.3

[1] Estimated initial value in the smectic A phase (initial time).

Therefore, it appears that one of the driving forces that stabilizes ionic liquid crystals in the smectic phase is an increased electrostatic interaction that can be obtained, for example, by using smaller anions with a higher charge density. The same qualitative result, as mentioned in the Introduction, was obtained by using a coarse-grained force-field of imidazolium salts, where the total charge of the cation head and anion was artificially varied from 0.7*e* up to 1.2*e* while keeping all the remaining parameters the same [48]. It was observed that the thermal range of stability of the ionic smectic phase was largely increased by increasing the charge of the ionic parts from about 50 K of thermal range of ionic smectic phase for an unscaled system (charges of the ions equal to +1.0*e* and −1.0*e*) up to more than 200 K of smectic range when the charge was scaled by a factor of 1.2. In contrast, the smectic phase disappeared for charges scaled by a factor smaller than 0.9. Moreover, the extended range was obtained as a result of a significant increase of the smectic-to-isotropic transition temperature, while the crystal-to-smectic transition temperature was very minorly affected by the charge. We note that a qualitatively similar observation holds for the studied salts which have a closer crystal-to-smectic transition temperature than the smectic-to-isotropic clearing point.

The results of these atomistic simulations are perfectly in agreement with the previous computational results of [48] and with the recent results, both by experiments and simulations, wherein the stability of the ionic smectic phase was compared for a series of methylpyridinium ILs based on halides and trihalides [47]. In fact, in that case it was also observed that increasing the size of the anion, while keeping the same cation, led to a decreased thermal range of stability of the ionic smectic phase.

5. Conclusions

In this paper we have compared two ionic liquid crystal systems, 1-dodecyl-3-methylimidazolium tetrafluoroborate ($[C_{12}C_1im][BF_4]$) and 1-dodecyl-3-methylimidazolium chloride ($[C_{12}C_1im]Cl$), by means of fully atomistic MD simulations. From a purely topological point of view, the two systems differ by the sizes of their anions (we can assume that the shape of the tetrafluoroborate, having a tetrahedral symmetry, is sufficiently close to spherical) and therefore by the anions' charge densities only.

In qualitative agreement with experimental observations, we find that the chloride systems exhibit a stable and highly ordered ionic smectic phase (the experimental salt has a thermal range of ionic

smectic phase of more than 100 K) while the tetrafluoroborate systems at the same temperature melt into an isotropic ionic liquid (the experimental systems have a small range of ionic smectic phase of just 12 K).

A comparison of the intermolecular energetic contributions of the two systems, Coulomb and van der Waals, reveals that the key factor that stabilizes the ionic smectic phase is an increased electrostatic contribution in the chloride salt due to a higher charge density (smaller size) of the chloride anion compared to the tetrafluoroborate anion. This increased interaction keeps the structure of the ionic layer and allows the hydrophobic region to be in a liquid-like state at the same time, preventing a complete melting into an isotropic system.

Funding: This research was funded by the CINECA-ISCRA, project number HP10CUVQ5Z, and by the CNR-CAS bilateral agreement 2017–2019. Additional computational resources were provided by the C3P Computational Community of the Department of Chemical Sciences of the University of Padova.

Conflicts of Interest: The author declares no conflict of interest.

References

1. Goossens, K.; Lava, K.; Bielawski, C.W.; Binnemans, K. Ionic Liquid Crystals: Versatile Materials. *Chem. Rev.* **2016**, *116*, 4643–4807. [CrossRef] [PubMed]
2. Fernandez, A.A.; Kouwer, P.H.J. Key Developments in Ionic Liquid Crystals. *Int. J. Mol. Sci.* **2016**, *17*, 731. [CrossRef] [PubMed]
3. Yuan, F.; Chi, S.; Dong, S.; Zou, X.; Lv, S.; Bao, L.; Wang, J. Ionic liquid crystal with fast ion-conductive tunnels for potential application in solvent-free Li-ion batteries. *Electrochimica Acta* **2019**, *294*, 249–259. [CrossRef]
4. Yamanaka, N.; Kawano, R.; Kubo, W.; Masaki, N.; Kitamura, T.; Wada, Y.; Watanabe, M.; Yanagida, S. Dye-Sensitized TiO_2 Solar Cells Using Imidazolium-Type Ionic Liquid Crystal Systems as Effective Electrolytes†. *J. Phys. Chem. B* **2007**, *111*, 4763–4769. [CrossRef] [PubMed]
5. Pan, X.; Wang, M.; Fang, X.; Zhang, C.; Huo, Z.; Dai, S. Ionic liquid crystal-based electrolyte with enhanced charge transport for dye-sensitized solar cells. *Sci. China Ser. B Chem.* **2013**, *56*, 1463–1469. [CrossRef]
6. Högberg, D.; Soberats, B.; Yatagai, R.; Uchida, S.; Yoshio, M.; Kloo, L.; Segawa, H.; Kato, T. Liquid-Crystalline Dye-Sensitized Solar Cells: Design of Two-Dimensional Molecular Assemblies for Efficient Ion Transport and Thermal Stability. *Chem. Mater.* **2016**, *28*, 6493–6500. [CrossRef]
7. Bowlas, C.J.; Bruce, D.; Seddon, K.R. Liquid-crystalline ionic liquids. *Chem. Commun.* **1996**, *14*, 1625. [CrossRef]
8. Bugaychuk, S.; Garbovskiy, Y.; Klimusheva, G.; Mirnaya, T.; Garbovskiy, Y. Novel materials based on metal-alkanoate liquid crystals and smectic glasses for impulse dynamic holographic applications. *Sect. Title Radiat. Chem. Photochem. Photogr. Other Reprogr. Process.* **2008**, 120–122.
9. Klimusheva, G.; Mirnaya, T.; Garbovskiy, Y.; Mirnaya, T. Versatile nonlinear-optical materials based on mesomorphic metal alkanoates: Design, properties, and applications. *Liq. Cryst. Rev.* **2015**, *3*, 28–57. [CrossRef]
10. Binnemans, K.; Van Deun, R.; Thijs, B.; Vanwelkenhuysen, I.; Geuens, I. Structure and Mesomorphism of Silver Alkanoates. *Chem. Mater.* **2004**, *16*, 2021–2027. [CrossRef]
11. Schlick, M.C.; Kapernaum, N.; Neidhardt, M.M.; Wöhrle, T.; Stöckl, Y.; Laschat, S.; Giesselmann, F.; Gießelmann, F. Large Electro-Optic Kerr Effect in Ionic Liquid Crystals: Connecting Features of Liquid Crystals and Polyelectrolytes. *ChemPhysChem* **2018**, *19*, 2305–2312. [CrossRef] [PubMed]
12. Cospito, S.; Beneduci, A.; Veltri, L.; Salamończyk, M.; Chidichimo, G. Mesomorphism and electrochemistry of thienoviologen liquid crystals. *Phys. Chem. Chem. Phys.* **2015**, *17*, 17670–17678. [CrossRef] [PubMed]
13. Beneduci, A.; Cospito, S.; La Deda, M.; Chidichimo, G. Fluorescent Materials: Highly Fluorescent Thienoviologen-Based Polymer Gels for Single Layer Electrofluorochromic Devices (Adv. Funct. Mater. 8/2015). *Adv. Funct. Mater.* **2015**, *25*, 1239. [CrossRef]
14. Pibiri, I.; Beneduci, A.; Carraro, M.; Causin, V.; Casella, G.; Corrente, G.A.; Chidichimo, G.; Pace, A.; Riccobono, A.; Saielli, G. Mesomorphic and electrooptical properties of viologens based on non-symmetric alkyl/polyfluoroalkyl functionalization and on an oxadiazolyl-extended bent core. *J. Mater. Chem. C* **2019**, *7*, 7974–7983. [CrossRef]

15. Beneduci, A.; Cospito, S.; La Deda, M.; Veltri, L.; Chidichimo, G. Electrofluorochromism in pi-conjugated ionic liquid crystals. *Nat. Commun.* **2014**, *5*, 3105. [CrossRef]
16. Veltri, L.; Maltese, V.; Auriemma, F.; Santillo, C.; Cospito, S.; La Deda, M.; Chidichimo, G.; Gabriele, B.; De Rosa, C.; Beneduci, A. Mesophase Tuning in Discotic Dimers π-Conjugated Ionic Liquid Crystals through Supramolecular Interactions and the Thermal History. *Cryst. Growth Des.* **2016**, *16*, 5646–5656. [CrossRef]
17. Veltri, L.; Cavallo, G.; Beneduci, A.; Metrangolo, P.; Corrente, G.A.; Ursini, M.; Romeo, R.; Terraneo, G.T.; Gabriele, B. Synthesis and thermotropic properties of new green electrochromic ionic liquid crystals. *New J. Chem.* **2019**, *43*, 18285–18293. [CrossRef]
18. Wuckert, E.; Harjung, M.D.; Kapernaum, N.; Mueller, C.; Frey, W.; Baro, A.; Giesselmann, F.; Laschat, S. Photoresponsive ionic liquid crystals based on azobenzene guanidinium salts. *Phys. Chem. Chem. Phys.* **2015**, *17*, 8382–8392. [CrossRef]
19. Butschies, M.; Frey, W.; Laschat, S. Designer Ionic Liquid Crystals Based on Congruently Shaped Guanidinium Sulfonates. *Chem. - A Eur. J.* **2012**, *18*, 3014–3022. [CrossRef]
20. Sauer, S.; Saliba, S.; Tussetschläger, S.; Baro, A.; Frey, W.; Giesselmann, F.; Laschat, S.; Kantlehner, W. p-Alkoxybiphenyls with guanidinium head groups displaying smectic mesophases. *Liq. Cryst.* **2009**, *36*, 275–299. [CrossRef]
21. Goossens, K.; Lava, K.; Nockemann, P.; Van Hecke, K.; Van Meervelt, L.; Pattison, P.; Binnemans, K.; Cardinaels, T. Pyrrolidinium Ionic Liquid Crystals with Pendant Mesogenic Groups. *Langmuir* **2009**, *25*, 5881–5897. [CrossRef] [PubMed]
22. Causin, V.; Saielli, G. Effect of asymmetric substitution on the mesomorphic behaviour of low-melting viologen salts of bis(trifluoromethanesulfonyl)amide. *J. Mater. Chem.* **2009**, *19*, 9153. [CrossRef]
23. Bhowmik, P.; Han, H.; Nedeltchev, I.; Cebe, J. Room-Temperature Thermotropic Ionic Liquid Crystals: Viologen Bis(Triflimide) Salts. *Mol. Cryst. Liq. Cryst.* **2004**, *419*, 27–46. [CrossRef]
24. Asaftei, S.; Ciobanu, M.; Lepadatu, A.M.; Enfeng, S.; Beginn, U. Thermotropic ionic liquid crystals by molecular-assembly and ion pairing of 4,4′-bipyridinium derivatives and tris(dodecyloxy)benzenesulfonats in a non-polar solvent. *J. Mater. Chem.* **2012**, *22*, 14426–14437. [CrossRef]
25. Casella, G.; Causin, V.; Rastrelli, F.; Saielli, G. Viologen-based ionic liquid crystals: Induction of a smectic A phase by dimerisation. *Phys. Chem. Chem. Phys.* **2014**, *16*, 5048–5051. [CrossRef] [PubMed]
26. Casella, G.; Causin, V.; Rastrelli, F.; Saielli, G. Ionic liquid crystals based on viologen dimers: Tuning the mesomorphism by varying the conformational freedom of the ionic layer. *Liq. Cryst.* **2016**, *43*, 1161–1173. [CrossRef]
27. Kobayashi, T.; Ichikawa, T. Design of Viologen-Based Liquid Crystals Exhibiting Bicontinuous Cubic Phases and Their Redox-Active Behavior. *Materials (Basel)* **2017**, *10*, 1243. [CrossRef]
28. Bhowmik, P.K.; Killarney, S.T.; Li, J.R.A.; Koh, J.J.; Han, H.; Sharpnack, L.; Agra-Kooijman, D.M.; Fisch, M.R.; Kumar, S. Thermotropic liquid-crystalline properties of extended viologen bis(triflimide) salts. *Liq. Cryst.* **2017**, *45*, 872–885. [CrossRef]
29. Nelyubina, Y.; Shaplov, A.S.; Lozinskaya, E.; Buzin, M.I.; Vygodskii, Y.S. A New Volume-Based Approach for Predicting Thermophysical Behavior of Ionic Liquids and Ionic Liquid Crystals. *J. Am. Chem. Soc.* **2016**, *138*, 10076–10079. [CrossRef]
30. A Mirnaya, T.; Prisyazhnyi, V.D.; A Shcherbakov, V. The liquid-crystalline state of salt melts containing organic ions. *Russ. Chem. Rev.* **1989**, *58*, 821–834. [CrossRef]
31. Martinez-Casado, F.J.; Riesco, M.R.; Yelamos, M.I.R.; Arenas, A.S.; Cheda, J.A.R. The role of calorimetry in the structural study of mesophases and their glass states. *J. Therm. Anal. Calorim.* **2011**, *108*, 399–413. [CrossRef]
32. Mirnaya, T.A.; Yaremchuk, G.G.; Prisyazhnyi, V.D. Formation of smectic mesophases in binary systems of short chain alkanoic acid salts. *Liq. Cryst.* **1990**, *8*, 701–705. [CrossRef]
33. Quevillon, M.; Whitmer, J.K. Charge Transport and Phase Behavior of Imidazolium-Based Ionic Liquid Crystals from Fully Atomistic Simulations. *Materials (Basel)* **2018**, *11*, 64. [CrossRef] [PubMed]
34. Frezzato, D.; Saielli, G. Distribution and Dynamic Properties of Xenon Dissolved in the Ionic Smectic Phase of $[C_{16}mim][NO_3]$: MD Simulation and Theoretical Model. *J. Phys. Chem. B* **2016**, *120*, 2578–2585. [CrossRef] [PubMed]
35. Saielli, G. Fully Atomistic Simulations of the Ionic Liquid Crystal $[C_{16}mim][NO_3]$: Orientational Order Parameters and Voids Distribution. *J. Phys. Chem. B* **2016**, *120*, 2569–2577. [CrossRef] [PubMed]

36. Di Pietro, M.E.; Margola, T.; Celebre, G.; De Luca, G.; Saielli, G. A combined LX-NMR and molecular dynamics investigation of the bulk and local structure of ionic liquid crystals. *Soft Matter* **2019**, *15*, 4486–4497. [CrossRef]
37. Cao, W.; Wang, Y. Phase Behaviors of Ionic Liquids Heating from Different Crystal Polymorphs toward the Same Smectic-A Ionic Liquid Crystal by Molecular Dynamics Simulation. *Crystals* **2019**, *9*, 26. [CrossRef]
38. Schenkel, M.R.; Hooper, J.B.; Moran, M.J.; Robertson, L.; Bedrov, D.; Gin, D. Effect of counter-ion on the thermotropic liquid crystal behaviour of bis(alkyl)-tris(imidazolium salt) compounds. *Liq. Cryst.* **2014**, *41*, 1668–1685. [CrossRef]
39. Saielli, G.; Voth, G.A.; Wang, Y. Diffusion mechanisms in smectic ionic liquid crystals: Insights from coarse-grained MD simulations. *Soft Matter* **2013**, *9*, 5716. [CrossRef]
40. Saielli, G. MD simulation of the mesomorphic behaviour of 1-hexadecyl-3-methylimidazolium nitrate: Assessment of the performance of a coarse-grained force field. *Soft Matter* **2012**, *8*, 10279. [CrossRef]
41. Ji, Y.; Shi, R.; Wang, Y.; Saielli, G. Effect of the Chain Length on the Structure of Ionic Liquids: From Spatial Heterogeneity to Ionic Liquid Crystals. *J. Phys. Chem. B* **2013**, *117*, 1104–1109. [CrossRef] [PubMed]
42. Margola, T.; Satoh, K.; Saielli, G. Comparison of the Mesomorphic Behaviour of 1:1 and 1:2 Mixtures of Charged Gay-Berne GB(4.4,20.0,1,1) and Lennard-Jones Particles. *Crystals* **2018**, *8*, 371. [CrossRef]
43. Saielli, G.; Margola, T.; Satoh, K. Tuning Coulombic interactions to stabilize nematic and smectic ionic liquid crystal phases in mixtures of charged soft ellipsoids and spheres. *Soft Matter* **2017**, *13*, 5204–5213. [CrossRef] [PubMed]
44. Margola, T.; Saielli, G.; Satoh, K. MD simulations of mixtures of charged Gay-Berne and Lennard-Jones particles as models of ionic liquid crystals. *Mol. Cryst. Liq. Cryst.* **2017**, *649*, 50–58. [CrossRef]
45. Saielli, G.; Satoh, K. A coarse-grained model of ionic liquid crystals: The effect of stoichiometry on the stability of the ionic nematic phase. *Phys. Chem. Chem. Phys.* **2019**, *21*, 20327–20337. [CrossRef] [PubMed]
46. Ganzenmüller, G.C.; Patey, G.N. Charge Ordering Induces a Smectic Phase in Oblate Ionic Liquid Crystals. *Phys. Rev. Lett.* **2010**, *105*, 137801. [CrossRef]
47. Wang, Y.; Senthilkumar, B.; Causin, V.; Swamy, V.P.; Wang, Y.; Saielli, G.; Beeran, S.; Paul, V. Influence of the ion size on the stability of the smectic phase of ionic liquid crystals. *Soft Matter* **2020**, *16*, 411–420.
48. Saielli, G.; Wang, Y. Role of the Electrostatic Interactions in the Stabilization of Ionic Liquid Crystals: Insights from Coarse-Grained MD Simulations of an Imidazolium Model. *J. Phys. Chem. B* **2016**, *120*, 9152–9160. [CrossRef]
49. Bradley, A.E.; Hardacre, C.; Holbrey, J.D.; Johnston, S.; McMath, S.E.J.; Nieuwenhuyzen, M. Small-Angle X-ray Scattering Studies of Liquid Crystalline 1-Alkyl-3-methylimidazolium Salts. *Chem. Mater.* **2002**, *14*, 629–635. [CrossRef]
50. Holbrey, J.D.; Seddon, K.R. The phase behaviour of 1-alkyl-3-methylimidazolium tetrafluoroborates; ionic liquids and ionic liquid crystals. *J. Chem. Soc. Dalton Trans.* **1999**, *13*, 2133–2140. [CrossRef]
51. Smith, W.; Forester, T.R.; Todorov, I.T. DL_POLY Classic. 2010. Available online: www.ccp5.ac.uk/DL_POLY_CLASSIC (accessed on 27 March 2020).
52. Lopes, J.N.C.; Deschamps, J.; Padua, A.A.H.A.H. Modeling Ionic Liquids Using a Systematic All-Atom Force Field. *J. Phys. Chem. B* **2004**, *108*, 11250. [CrossRef]
53. Hoover, W.G. Canonical dynamics: Equilibrium phase-space distributions. *Phys. Rev. A* **1985**, *31*, 1695–1697. [CrossRef]
54. Melchionna, S.; Ciccotti, G.; Holian, B.L. Hoover NPT dynamics for systems varying in shape and size. *Mol. Phys.* **1993**, *78*, 533–544. [CrossRef]
55. Scott, R.; Allen, M.P.; Tildesley, D.J. Computer Simulation of Liquids. *Math. Comput.* **1991**, *57*, 442. [CrossRef]
56. Smith, W.; Forester, T. Parallel macromolecular simulations and the replicated data strategy. *Comput. Phys. Commun.* **1994**, *79*, 52–62. [CrossRef]
57. Ryckaert, J.-P.; Ciccotti, G.; Berendsen, H.J. Numerical integration of the cartesian equations of motion of a system with constraints: Molecular dynamics of n-alkanes. *J. Comput. Phys.* **1977**, *23*, 327–341. [CrossRef]
58. Humphrey, W.; Dalke, A.; Schulten, K. VMD: Visual molecular dynamics. *J. Mol. Graph.* **1996**, *14*, 33–38. Available online: http://www.ks.uiuc.edu/Research/vmd/ (accessed on 27 March 2020). [CrossRef]
59. Dommert, F.; Wendler, K.; Berger, R.; Site, L.D.; Holm, C. Force Fields for Studying the Structure and Dynamics of Ionic Liquids: A Critical Review of Recent Developments. *ChemPhysChem* **2012**, *13*, 1625–1637. [CrossRef]

60. Bedrov, D.; Piquemal, J.-P.; Borodin, O.; MacKerell, A.D.; Roux, B.; Schröder, C. Molecular Dynamics Simulations of Ionic Liquids and Electrolytes Using Polarizable Force Fields. *Chem. Rev.* **2019**, *119*, 7940–7995. [CrossRef]
61. Di Pietro, M.E.; Celebre, G.; De Luca, G.; Zimmermann, H.; Cinacchi, G. Smectic order parameters via liquid crystal NMR spectroscopy: Application to a partial bilayer smectic A phase. *Eur. Phys. J. E* **2012**, *35*, 112. [CrossRef]
62. Youngs, T.G.A.; Hardacre, C. Application of Static Charge Transfer within an Ionic-Liquid Force Field and Its Effect on Structure and Dynamics. *ChemPhysChem* **2008**, *9*, 1548–1558. [CrossRef] [PubMed]
63. Zhong, X.; Liu, Z.; Cao, D. Improved Classical United-Atom Force Field for Imidazolium-Based Ionic Liquids: Tetrafluoroborate, Hexafluorophosphate, Methylsulfate, Trifluoromethylsulfonate, Acetate, Trifluoroacetate, and Bis(trifluoromethylsulfonyl)amide. *J. Phys. Chem. B* **2011**, *115*, 10027–10040. [CrossRef] [PubMed]
64. Matsumiya, M.; Hata, K.; Tsunashima, K. Self-diffusion behaviors of ionic liquids by MD simulation based on united-atom force field introduced charge scaling by ab initio MO simulation. *J. Mol. Liq.* **2015**, *203*, 125–130. [CrossRef]
65. Schröder, C. Comparing reduced partial charge models with polarizable simulations of ionic liquids. *Phys. Chem. Chem. Phys.* **2012**, *14*, 3089. [CrossRef]